

# Effects of Crossover Operators on Genetic Algorithms for the Extraction of Solar Cell Parameters from Noisy Data

**Ibtissam Tebbal**

Department of Electronics, Laboratory of Optoelectronics and Components, University of Ferhat Abbas Setif 1, Algeria  
ibtiss08@yahoo.fr (corresponding author)

**Abdelhak Ferhat Hamida**

Department of Electronics, Laboratory of Optoelectronics and Components, University of Ferhat Abbas Setif 1, Algeria  
a\_ferhat\_h@yahoo.fr

Received: 28 January 2023 | Revised: 12 March 2023 | Accepted: 16 March 2023

Licensed under a CC-BY 4.0 license | Copyright (c) by the authors | DOI: <https://doi.org/10.48084/etasr.5417>

## ABSTRACT

This study analyzed the accuracy of solar cell modeling parameters extracted from noisy data using Genetic Algorithms (GAs). Three crossover operators (XOs) were examined, namely the Uniform (UXO), Arithmetic (AXO), and Blend (BXO) operators. The data used were an experimental benchmark cell and a simulated curve where noise levels ( $p$ ) from 0 to 10% were added. For each XO, the analysis was carried out by running GAs 100 times and varying  $p$  and population size ( $N_{pop}$ ). Simulation results showed that UXO and AXO suffered from premature convergence and failed to provide parameters with good precision even with very high  $N_{pop}$ , although they provided good fitting. In all analyzed cases, BXO outperformed UXO and AXO and the results showed that it can compete with the most efficient methods. For the benchmark curve, BXO reproduced the best RMSE found in the literature (0.7730062 mA) while providing the exact values of the parameters and a very low RMSE (1E-13) for the clean curve ( $p=0$ ). For noisy curves, the errors of the extracted parameters were smaller than 10% for  $p$  lower than or equal to 6%. For higher values of  $p$ , the errors were smaller than 30%.

*Keywords-solar cells; parameter extraction; genetic algorithms; crossover operators*

## I. INTRODUCTION

The current-voltage ( $I$ - $V$ ) characteristic of a Solar Cell (SC) is often predicted by the Single Diode Model (SDM) [1]:

$$I = I_{ph} - I_s \left[ e^{(V+R_s I) / nV_{th}} - 1 \right] - G_p (V + R_s I) \quad (1)$$

where  $V_{th} = kT/q$  is the thermal voltage,  $T$  is the temperature,  $k$  is the Boltzmann constant, and  $q$  is the elementary charge. The photocurrent  $I_{ph}$ , the reverse saturation current  $I_s$ , the ideality factor  $n$ , the series resistance  $R_s$ , and the parallel conductance  $G_p$  are SDM parameters that are commonly supposed constants independent of temperature and voltage. The non-linear nature of this equation makes the extraction of SDM parameters from  $I$ - $V$  characteristics a very hard task. Since the '60s, many methods have been proposed [1-12]. Despite their huge number, none is wholly satisfactory and there is a need and a challenge to propose new methods. The proposed methods are either analytical or numerical [12-13]. The analytical methods, mainly published before 2000, often operate in specified regions of  $I$ - $V$  curves and require prior knowledge of some

defined points, such as the short-circuit current  $I_{sc}$ , the open-circuit voltage  $V_{oc}$ , the current  $I_m$ , and the voltage  $V_m$  at the maximum power point [13]. The numerical methods are based on deterministic or Metaheuristic Optimization Algorithms (MOAs) that process over the whole curve and do not require any specified points. Deterministic algorithms are based on initial conditions, require curve derivatives, and do not guarantee a global solution. These drawbacks were overcome by MOAs [14], where evolutionary algorithms (EAs) constitute an important subclass. Hence, they are increasingly used in SC parameter estimation [1, 4]. Despite the huge number of proposed methods, only a few deal with the effects of noise levels on the extracted parameters [9-13, 15, 16]. This is an important issue, since noise is always present in the measured data and may vary with environmental conditions. Only [12] and [13], by proposing a least squares-based method and four metaheuristic-based methods, namely, the Self-Adaptive Differential Evolution algorithm (SADE), the Performance Guided JAYA algorithm (PGJAYA), the Self-Adaptive Teaching-Learning-based Optimization algorithm (SATLBO), and the Biogeography-based Heterogeneous Cuckoo Search

algorithm (BHCS), respectively, evaluated in-depth the effect of noise on the extracted parameters. These studies investigated the effect of noise levels from 0 to 10% on each method and parameter. In addition, in [13], the performance of the methods was analyzed by varying the population size.

This study investigated the effects of noise on the extracted parameters of SCs using GAs, compared 3 distinct crossover operators (XOs), and showed that the performance depends on the chosen XO. Experimental and synthetic noisy and noise-free curves were used. The study of the effects of XO on GAs applied to the extraction of SDM from noisy curves has not been considered before.

II. PROBLEM FORMULATION

The SC parameter estimation problem is formulated as finding a vector  $P=(I_{ph}, I_s, n, R_s, G_p)$  such that  $N$  synthetic data  $(I_{s,i}, V_i)$ , generated with the SDM (1), fit the experimental ones  $(I_{e,i}, V_i)$ . The problem is solved by minimizing an Objective Function (OF) that calculates the error between the experimental and synthetic data. This study used the Root Mean Square Estimation (RMSE) defined by (2) as OF, which is the most used in fitting problems [1-12]:

$$RMSE = \sqrt{\frac{1}{N} \sum_{i=1}^N [I_{e,i} - I_{s,i}]^2} \tag{2}$$

III. GENETIC ALGORITHM TUNING

Since their introduction in [17], GAs have been increasingly studied, developed, and used in solving complex problems in science and engineering [18-19], machine learning [20], economics and finance [21], VLSI design [22], embedded system design [23], and others [24-25]. GAs are metaheuristic methods that mimic Darwin’s natural selection principles and genetics, that is, survival of the fittest [14, 26], and use selection, mutation, and crossover genetic-like operators. When using GAs, decisions have to be made on the stopping condition, the alphabet used, the population size, the genetic operators, and the corresponding probabilities to use. The program was set to stop when either it reached 20000 generations or all solutions in the population were in a prescribed standard deviation of  $10^{-12}$ . Real coding (RCGA) was used to provide good resolution, where each chromosome was a  $P$  vector with the SDM parameters. The selection and mutation operators were set to the 'roulette wheel' and 'Gaussian', respectively, and the probabilities were fixed to  $p_{cross}=0.9$  and  $p_{mut}=0.01$  for the crossover and the mutation operators, respectively. The population size was taken as a variable in the range of [20, 20000]. Since GAs are considered to get their power from the XO [27-28], three widely used XOs were compared: the uniform, the arithmetic, and the blend operators [29-31].

A. Uniform Operator

The Uniform crossover operator (UXO) is inherited from binary coding and was historically the first one to be used [26]. When two chromosomes are crossed, each gene of the offspring randomly comes from the first or the second parent. When used with RCGA, UXO does not create new values of

genes other than those initially created. Only mutation can do this.

B. Arithmetic Operator

Given two parents  $x$  and  $y$  with genes  $x_i$  and  $y_i$ , respectively, and  $\alpha_i$  in  $[0, 1]$ , the Arithmetic crossover operator (AXO) creates two offsprings  $z$  and  $w$  whose genes  $z_i$  and  $w_i$  are:

$$\begin{aligned} z_i &= \alpha_i x_i + (1 - \alpha_i) y_i \\ w_i &= \alpha_i y_i + (1 - \alpha_i) x_i \end{aligned} \tag{3}$$

where  $\alpha_i$  are either uniform random numbers or constants in uniform and non-uniform AXO, respectively. AXO reduces the range of gene values in the population.

C. Blend Operator

Given  $d_i=abs(x_i-y_i)$  and a fixed  $\alpha$ , usually 0.5, the Blend crossover operator (BXO) creates an offspring  $U$  whose genes are uniform random numbers in the interval  $U_i$  given by [32]:

$$U_i = [min(x_i, y_i) - \alpha d_i, max(x_i, y_i) + \alpha d_i] \tag{4}$$

BXO enlarges the range of gene values in the population.

IV. COMPUTATIONAL PROCEDURE

The GAs were coded in C++ using the GALib library [33], and applied to the experimental and the synthetic versions of the most used benchmark  $I-V$  curve [34]: a 57mm diameter crystalline silicon SC from RTC France, operating at 33°C and 1000W/m<sup>2</sup>. The synthetic version was simulated with (1) in the voltage range of [0-0.6V] using the parameters of [13], shown in Table I, along with the restricted search intervals. Since the exact values are known, the convergence can be easily analyzed. To study the effect of noise on the extracted parameters, an artificial noise was added to the synthetic curve [9, 12-13, 15, 35]:

$$I_{noisy} = I_{syn} \times (1 + p \times rand) \tag{5}$$

where  $I_{noisy}$  is the noisy current,  $I_{syn}$  is the synthetic noise-free current,  $rand$  is a random number between -1 and +1, and  $p$  is the noise level from 0 to 10%, to be added. For each XO considered, GAs were run by varying  $p$  and  $N_{pop}$ . To obtain a statistical evaluation, 100 GA runs were executed for each pair  $(p, N_{pop})$ , and the best solution and related parameters (RMSE,  $P$ ) were saved for each run. The parameter values corresponding to the best RMSE on the 100 runs were then selected as the solution. Two other important quantities, the absolute ( $\Delta$ ) and the relative error ( $\Delta_B$ ) between the exact and the best values, respectively, were also computed.

TABLE I. EXACT VALUES AND SEARCH INTERVALS OF THE PARAMETERS APPLIED TO GA

|              | $I_{ph}$ (A) | $I_s$ (μA) | $n$    | $R_s$ (Ω) | $G_p$ (Ω <sup>-1</sup> ) |
|--------------|--------------|------------|--------|-----------|--------------------------|
| <b>Exact</b> | 0.7608       | 0.3223     | 1.4808 | 0.0367    | 0.0173                   |
| <b>Low</b>   | 0.0000       | 0.1000     | 1.0000 | 0.0001    | 0.0001                   |
| <b>High</b>  | 1.0000       | 1.0000     | 2.0000 | 1.0000    | 1.0000                   |

V. RESULTS AND DISCUSSION

This section presents the results of applying GAs to the parameter extraction of the noise-free and noisy curves and the benchmark cell considering the three XOs.

A. Synthetic Curve

1) Noise-Free Curve

Figure 1 shows the RMSE obtained for the 3 considered XOs as a function of  $N_{pop}$ . According to [13], a good RMSE for this SC should be smaller than  $9.86022 \times 10^{-4}$ . As such, the fittings obtained by using BXO with all  $N_{pop}$  and UXO and AXO with  $N_{pop}$  of at least 150 and 100, respectively, are good. For UXO and AXO, the RMSE achieved was not less than  $2 \times 10^{-5}$  and  $2 \times 10^{-4}$ , respectively, while for BXO it steeply decreased to smaller values by several orders of magnitude:  $5 \times 10^{-4}$ ,  $2 \times 10^{-5}$ ,  $2 \times 10^{-8}$ ,  $1 \times 10^{-13}$ , and  $2 \times 10^{-16}$  for  $N_{pop}=20, 50, 100, 150,$  and  $20000,$  respectively. Running GAs using BXO with  $N_{pop}=50$  gives an equivalent performance to using UXO with  $N_{pop}=20000$ . For greater  $N_{pop}$ , BXO outperformed UXO and AXO. However, BXO converges very slowly, in more than 2000 iterations. On the other hand, UXO and AXO perform between 45 and 200 iterations until convergence is reached. The fast convergence to a non-optimal value and the slow decrease of the RMSE indicate that these XOs favor premature convergence. UXO does not create new genes other than those initially generated, and AXO does not explore the space outside the parents. The iterations quickly reach a state where there is no population diversity. Several techniques have been proposed to avoid premature convergence, but their study is beyond the scope of this work.

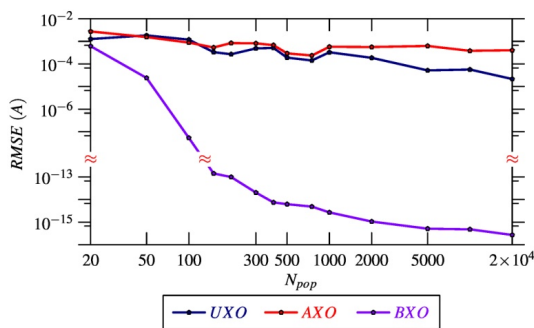


Fig. 1. RMSE of the noise-free curve as a function of population size ( $N_{pop}$ ) for the three crossover operators.

a) The UXO Operator

Figure 2 shows the relative error  $\Delta_B$  of the extracted parameters as a function of  $N_{pop}$  and the slow increase of precision (decrease of the error) as  $N_{pop}$  increases.  $I_{ph}$  is the parameter extracted with the highest precision, followed, in not less than one order of magnitude away, by  $n, R_s, G_p,$  and  $I_s$ . With  $N_{pop}$  greater than 150, the errors were always smaller than 20%, and for 20000 they were smaller than 0.4%. This corresponds to the region where the RMSE was less than  $1 \times 10^{-3}$ %. This increase is ascribed to the increase in the resolution of the initial population. Better performance can be achieved by increasing  $N_{pop}$  at the expense of huge memory space and execution time. Despite these results, a smaller

RMSE was expected since the exact parameter values were known and the noise-free data. It was expected to get all the Significant Digits (SDs) of the parameters given in Table I to generate the curve using (1). Such performance can be easily obtained with the Newton-Raphson method. Given the values and precision of each parameter, it can be easily shown that the errors must be smaller than  $6.5 \times 10^{-3}\%, 1.5 \times 10^{-2}\%, 3.3 \times 10^{-3}\%, 0.14\%,$  and  $0.29\%$  for  $I_{ph}, I_s, n, R_s,$  and  $G_p,$  respectively, to extract all SDs of each parameter. So, each error must be smaller than  $3.3 \times 10^{-3}\%$  to extract all SDs from the 5 parameters. This can be verified in Table II which shows the RMSE, the extracted parameters, and the errors obtained with  $N_{pop}=100, 1000,$  and  $20000$ . A comparison of Tables I and II shows that for  $N_{pop}=20000,$  the extracted parameters were close to the exact values. However, there is a lack of precision since, although all SDs of  $I_{ph}$  and  $R_s$  were found, there was a loss of two SDs for  $I_s$  and  $n$  and one for  $G_p$ . For more practical cases, i.e.  $N_{pop}=100$  and  $1000,$  all SDs were lost for  $I_s$  and 2 were lost for  $I_{ph}, R_s,$  and  $G_p$ . For  $n,$  4 and 3 SDs were lost for  $N_{pop}$  values of 100 and 1000. Despite this lack of precision, a good fit was obtained and all RMSEs for  $N_{pop}$  greater than 150 were better than the value of  $9.86022 \times 10^{-4}$  found in [13].

TABLE II. RESULTS FOR NOISE-FREE CURVE USING UXO

| $N_{pop}$          | 100      |                | 1000     |                | 20000    |                |
|--------------------|----------|----------------|----------|----------------|----------|----------------|
| Param              | Value    | $\Delta_B(\%)$ | Value    | $\Delta_B(\%)$ | Value    | $\Delta_B(\%)$ |
| $I_{ph}(A)$        | 0.76156  | 9.99E-2        | 0.76102  | 2.87E-2        | 0.76082  | 2.75E-3        |
| $I_s(\mu A)$       | 0.56704  | 75.94          | 0.26864  | 16.65          | 0.32390  | 0.4978         |
| $n$                | 1.54066  | 4.043          | 1.46262  | 1.228          | 1.48131  | 3.47E-2        |
| $R_s(\Omega)$      | 0.03419  | 7.011          | 0.03736  | 1.614          | 0.03673  | 8.29E-2        |
| $G_p(\Omega^{-1})$ | 0.01839  | 6.190          | 0.01609  | 10.25          | 0.01738  | 0.3698         |
| RMSE               | 1.193E-3 |                | 3.287E-4 |                | 2.154E-5 |                |

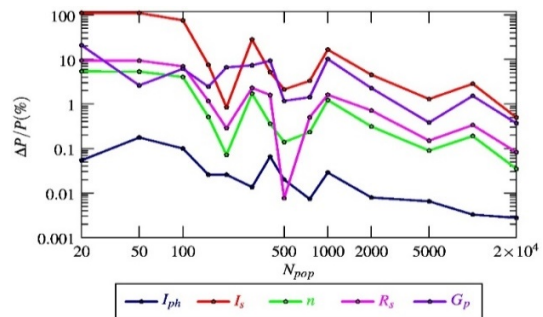


Fig. 2. Errors of the extracted model parameters of the synthetic noise-free solar cell as a function of the population size for the UXO operator.

b) The AXO Operator

Figure 3 shows  $\Delta_B$  as a function of  $N_{pop}$ .  $I_{ph}$  was extracted with the highest precision, followed by  $n, R_s, G_p,$  and  $I_s$  at several orders of magnitude away. The precision increased very slowly with increasing  $N_{pop}$  and the errors were smaller than 50% only for  $N_{pop}$  greater than 500. Figure 1 shows that the RMSE was less than  $1 \times 10^{-3}$  for  $N_{pop}$  greater than 100. The effect of premature convergence was stronger and the precision of the extracted parameters was lower than in UXO. Table III shows the RMSE, the extracted parameters, and the errors obtained with  $N_{pop}=100, 1000,$  and  $20000,$  where there was a lack of precision, although all RMSEs were good. Although 3 SDs were found for  $I_{ph},$  all SDs of  $I_s$  were lost, and only 1 was found for the other parameters.

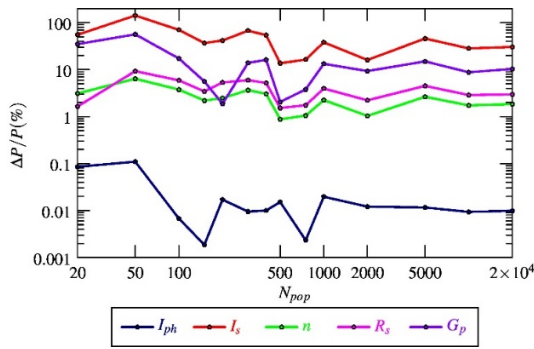


Fig. 3. Errors of the extracted model parameters of the synthetic noise-free solar cell as a function of the population size for the AXO operator.

TABLE III. RESULTS FOR NOISE-FREE CURVE USING AXO

| $N_{pop}$          | 100      |                | 1000     |                | 20000    |                |
|--------------------|----------|----------------|----------|----------------|----------|----------------|
| Param              | Value    | $\Delta_B(\%)$ | Value    | $\Delta_B(\%)$ | Value    | $\Delta_B(\%)$ |
| $I_{ph}(A)$        | 0.76085  | 6.75E-3        | 0.76065  | 1.97E-2        | 0.76072  | 9.90E-3        |
| $I_s(\mu A)$       | 0.54841  | 70.15          | 0.44515  | 38.12          | 0.42017  | 30.37          |
| $n$                | 1.53643  | 3.7570         | 1.51404  | 2.2446         | 1.5081   | 1.845          |
| $R_s(\Omega)$      | 0.03460  | 5.908          | 0.03531  | 3.959          | 0.03568  | 2.969          |
| $G_p(\Omega^{-1})$ | 0.01433  | 17.27          | 0.01501  | 13.30          | 0.01553  | 10.33          |
| RMSE               | 8.780E-4 |                | 5.766E-4 |                | 4.047E-5 |                |

c) The BXO Operator

Figure 4 shows that the  $\Delta_B$  of the extracted parameters using BXO was less than 1% for all considered  $N_{pop}$ .  $I_{ph}$  was the parameter extracted with the highest precision, as its corresponding error was always lower than  $1 \times 10^{-3}\%$ , and for  $N_{pop}$  greater than 400 it was 0% (it was set  $1 \times 10^{-15}\%$  in Figure 4 for the sake of logarithmic scale). This parameter was followed, not less than one order of magnitude away, by  $n$ ,  $R_s$ ,  $G_p$ , and  $I_s$ . The increase of precision was very fast as  $N_{pop}$  increased from 20 to 400. The error of  $I_s$  decreased from 1% to  $1 \times 10^{-11}\%$ . When  $N_{pop}$  increased from 400 to 20000, the precision slowly increased and the error of  $I_s$  decreased from  $1 \times 10^{-11}$  to  $1 \times 10^{-13}\%$ . The errors obtained, less than 1%, show that for  $N_{pop}$  as low as 20, at least one SD was found for each parameter. For  $N_{pop}=100$ , the absolute errors were  $1.31 \times 10^{-6}\%$ ,  $1.88 \times 10^{-3}\%$ ,  $5.92 \times 10^{-4}\%$ ,  $2.39 \times 10^{-5}\%$ , and  $3.62 \times 10^{-5}\%$  for  $I_{ph}$ ,  $I_s$ ,  $n$ ,  $R_s$ , and  $G_p$ , respectively. This is only a loss of two SDs in  $I_s$  and one in  $n$ . For  $N_{pop}$  greater than or equal to 150, all SDs of the parameters were exact in each GA execution.

TABLE IV. RESULTS FOR NOISE-FREE CURVE USING BXO

| $N_{pop}$          | 150       |                | 1000      |                | 20000     |                |
|--------------------|-----------|----------------|-----------|----------------|-----------|----------------|
| Error              | $\Delta$  | $\Delta_B(\%)$ | $\Delta$  | $\Delta_B(\%)$ | $\Delta$  | $\Delta_B(\%)$ |
| $I_{ph}(A)$        | 9.4E-15   | 1.2E-12        | 0.0000    | 0.0000         | 0.000     | 0.000          |
| $I_s(\mu A)$       | 1.1E-11   | 3.55E-9        | 6.7E-11   | 2.1E-12        | 5.6E-12   | 1.7E-13        |
| $n$                | 3.6E-12   | 2.4E-10        | 2.1E-11   | 1.4E-13        | 1.7E-12   | 1.2E-14        |
| $R_s(\Omega)$      | 1.5E-13   | 4.1E-10        | 8.7E-13   | 2.4E-13        | 7.0E-14   | 1.9E-14        |
| $G_p(\Omega^{-1})$ | 2.3E-13   | 1.38E-9        | 1.6E-12   | 9.3E-13        | 1.7E-13   | 1.0E-13        |
| RMSE               | 1.418E-10 |                | 2.686E-15 |                | 2.695E-16 |                |

Table IV shows the RMSE,  $\Delta$ , and  $\Delta_B$  of the extracted parameters for  $N_{pop}=150, 1000,$  and  $20000$ . The maximum  $\Delta$  ( $1.14E-11$ ), was seven positions away from the last SD of  $I_s$ . Hence, increasing  $N_{pop}$  to over 150 did not improve the precision. Figure 1 shows that running GAs using BXO with

$N_{pop}=50$  gave equivalent RMSEs as using UXO with  $N_{pop}=20000$ . Figures 2-4 for these  $N_{pop}$  show that BXO had better precision, and outperformed UXO and AXO with  $N_{pop}=150$ .

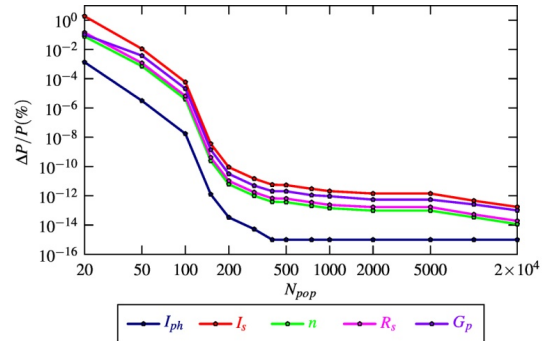


Fig. 4. Errors of the extracted model parameters of the synthetic noise-free solar cell as a function of the population size for the BXO operator.

d) Comments

The precision of the SC parameters extracted by GAs from noise-free data was greatly affected by the XO used. As reported in [36], obtaining a good fit, a synonym for good RMSE, does not prove the validity of the model parameters. Parameter extraction can have many purposes. If the goal is a good fitting regardless of the parameter precision, GAs can be run several times either by using BXO with a very low  $N_{pop}$ , such as 20, or by using UXO or AXO with a low  $N_{pop}$ , such as 150, and pick the best solution. If the goal is good precision ( $\Delta_B < 10\%$ ), GAs can be run several times using UXO with a high  $N_{pop}$ , such as 2000, and pick the best solution. If the goal is a high parameter precision ( $\Delta_B < 1\%$ ), GAs can be run using UXO several times with a very high  $N_{pop}$ , such as 20000, and pick the best solution. For all purposes, GAs can be run only once using BXO with a relatively low  $N_{pop}$ , such as 150, and get very good fitting and parameter precision. AXO gives parameters with very low precision for all  $N_{pop}$ , and can only be used for good fitting.

2) Noisy Curve

A noise level  $p$  varying from 0.1 to 10% was added to the synthetic curve using (5). The parameters of the noisy curves were extracted by GAs using UXO, AXO, and BXO. For all cases, the solutions were picked as the best over 100 runs of GAs.

a) The UXO and AXO Operators

Figures 5 and 6 show the errors of the parameters extracted by the GAs with  $N_{pop}=20000$  using UXO and AXO, respectively, as a function of noise levels. The errors were independent of noise levels for all  $N_{pop}$  values. For the two XOs,  $I_{ph}$  was the parameter extracted with the highest precision for all noise levels, with errors less than 1.2% and 0.5% for UXO and AXO, respectively. Although the errors were acceptable for  $R_s$  and  $n$ , with 14% and 7% for UXO and AXO, respectively, they reached very high values for  $G_p$  and  $I_s$ . The  $I_s$  and  $G_p$  values were 120% and 210% for UXO and 45% and

80% for AXO, respectively. Therefore, AXO performed better than UXO.

b) The BXO Operator

Figure 7 shows the results obtained with GA using BXO with  $N_{pop}=250$  as a function of  $p$ , where the errors increased with  $p$ . All errors were lower than 10%, except for  $I_s$  which reached 30% for  $p$  more than 6%. The errors of  $I_{ph}$ ,  $n$ ,  $R_s$ , and  $G_p$  were always less than 0.1%, 2%, 2%, and 10%, respectively. For practical cases with  $p$  less than 5%, all errors were less than 10%. Thus, BXO outperformed AXO and UXO for noisy curves.

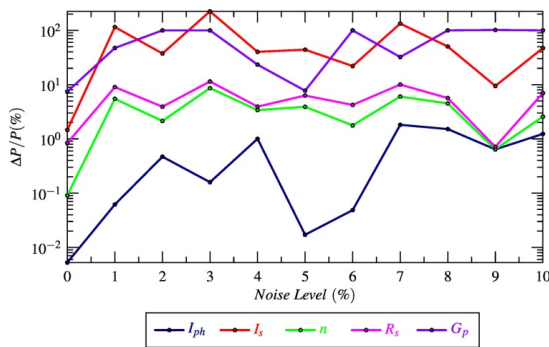


Fig. 5. Errors of the model parameters of the noisy synthetic solar cell as a function of the noise level for the UXO operator and  $N_{pop}=20000$ .

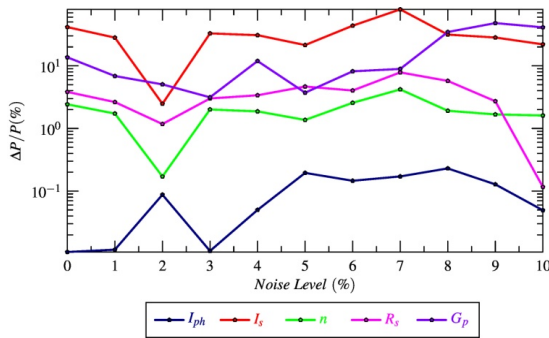


Fig. 6. Errors of the model parameters of the noisy synthetic solar cell as a function of the noise level for the AXO operator and  $N_{pop}=20000$ .

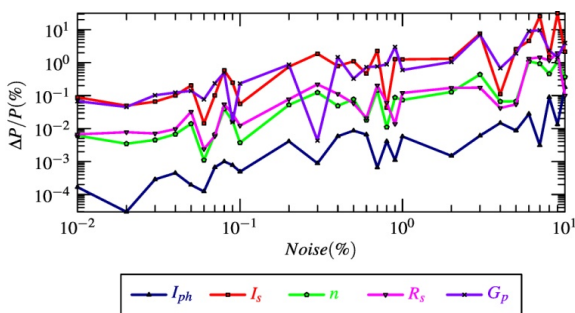


Fig. 7. Errors of the model parameters of the noisy synthetic solar cell as a function of the noise level for the BXO operator and  $N_{pop}=250$ .

c) Curve Fitting

Figures 8-10 show the noisy curves corresponding to  $p=1, 2, 5,$  and  $10\%$ , along with the corresponding fitting curves by

UXO, AXO, and BXO. Comparing the curves with the synthetic curve ( $p=0\%$ ) shows the good fit obtained by AXO and BXO. In the region  $I_{sc}-I_m$ , UXO gave a less good fit, which is acceptable only when considering that the curves are noisy.

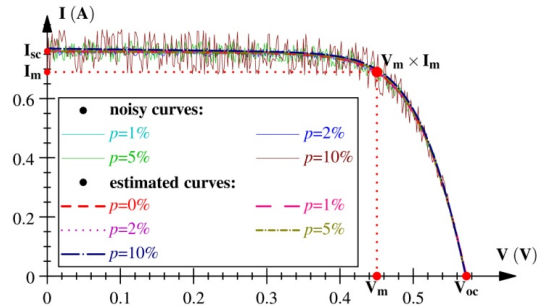


Fig. 8. Noisy synthetic data and corresponding fitted curves with parameters extracted by using UXO with  $N_{pop}=20000$ .

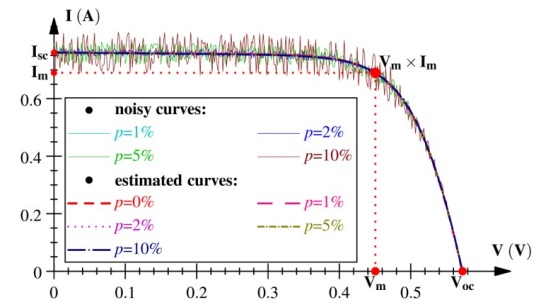


Fig. 9. Noisy synthetic data and corresponding fitted curves with parameters extracted by using AXO with  $N_{pop}=20000$ .

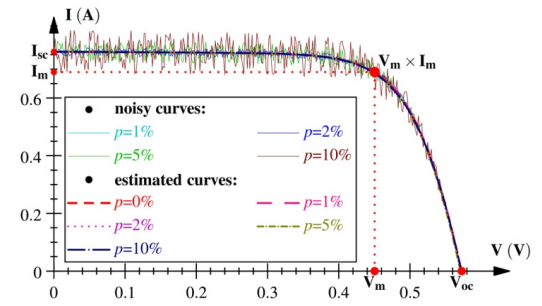


Fig. 10. Noisy synthetic data and corresponding fitted curves with parameters extracted by using BXO with  $N_{pop}=250$ .

d) Comments

For the noise-free curve, the quality of fit and the precision of parameters extracted by GAs were highly affected by the used XO. While AXO and BXO give good fitting, only BXO gives good parameter precision. For UXO, neither the fitting nor the parameter precision is good.

B. Experimental Data

The GAs were applied to the parameter extraction of the most used SC in the literature [34]. Table V shows the optimal obtained results along with those of some recently published studies, namely Grouping-based Global Harmony Search

(GGHS) and Innovative Global Harmony Search (IGHS) [37], Self-Adaptive Differential Evolution (SADE), Performance Guided JAYA (PGJAYA), and Self-Adaptive Teaching-Learning-based Optimization (SATLBO) [13], and Differential Evolution with Dynamic Control Factors (DEDCE) [38]. Figure 11 shows the obtained fitting.

The results of UXO and AXO were obtained with  $N_{pop}=20000$  and were very close to those of BXO. However, they were obtained only once in all GAs runs, and there is no guarantee that they will be reproduced in other runs. AXO gave better results than those of [13] and [37], but worse than BXO, due to the strong effect of premature convergence.

TABLE V. PARAMETERS EXTRACTED BY DIFFERENT METHODS

| Work                       | $I_{ph}(A)$ | $I_s(\mu A)$ | $n$    | $R_s(\Omega)$ | $G_p(\Omega^{-1})$ | RMSE ( $\times 10^{-4}A$ ) |
|----------------------------|-------------|--------------|--------|---------------|--------------------|----------------------------|
| This work                  |             |              |        |               |                    |                            |
| BXO                        | 0.7608      | 0.3107       | 1.4773 | 0.0365        | 0.0189             | 7.73006                    |
| UXO                        | 0.7606      | 0.3059       | 1.4757 | 0.0367        | 0.0181             | 7.87296                    |
| AXO                        | 0.7606      | 0.4455       | 1.5143 | 0.0349        | 0.0157             | 9.65930                    |
| Previous works             |             |              |        |               |                    |                            |
| GGHS [37]                  | 0.7609      | 0.3262       | 1.4822 | 0.0363        | 0.0188             | 9.9097                     |
| Fébbba [13] <sup>(a)</sup> | 0.7068      | 0.3230       | 1.4812 | 0.0364        | 0.0537             | 9.8602                     |
| DEDCE [38]                 | 0.7608      | 0.3107       | 1.4767 | 0.0365        | 0.0189             | 7.73006                    |
| IGHS [37]                  | 0.7608      | 0.3435       | 1.4874 | 0.0361        | 0.0188             | 9.9306                     |

a: DE, PGJAYA, and SATLBO [13]

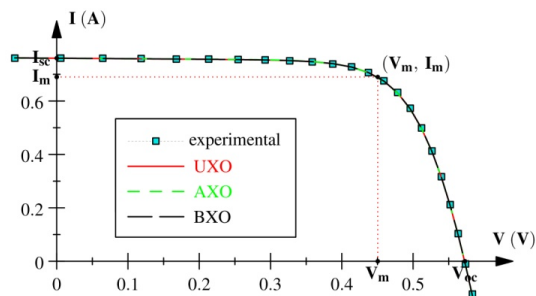


Fig. 11. Experimental data and fitted curves for the RTC solar cell.

BXO gave the same RMSE,  $I_{ph}$ ,  $I_s$ ,  $R_s$ , and  $G_p$  as DEDCE which had the smallest RMSE ( $7.730062 \times 10^{-4}$ ) for this SC [38]. There is only a small difference of 0.04% in the value of  $n$ , 1.4773 for BXO against 1.4767 for DEDCE. The concordance seems perfect. It can also be noticed that the results shown in Table V for BXO were reproduced in each GA run for all  $N_{pop}$  greater than or equal to 150 (1100 executions). Differences were observed only beyond the 7<sup>th</sup> SD. Hence, BXO outperforms UXO and AXO and competes with the most efficient methods.

VI. CONCLUSION

This study analyzed the accuracy of the 5 SDM parameters of SCs using GAs by considering the effect of 3 XOs, namely the UXO, the AXO, and the BXO. Three datasets were used, an experimental benchmark cell and simulated curves with noise levels ( $p$ ) of 0-10%. The analysis was performed by varying  $N_{pop}$  from 20 to 20000. For each triplet (XO,  $p$ ,  $N_{pop}$ ), 100 GA runs were conducted and the solution was picked as the result

of the best run. The simulation results showed that the performance of GAs varied significantly with the employed XO. When using UXO or AXO with very high  $N_{pop}$  (as high as 20000), GAs only produced good accuracy in the two following cases:

- with UXO for the noise-free curve
- with AXO for the benchmark cell, obtaining an RMSE of  $7.87296 \times 10^{-4}$ . As this result was obtained only once in more than 1400 runs, there is no guarantee that it can be reproduced.

For all other cases, the parameter accuracy is very low, explicitly:

- with UXO, for noisy data and the benchmark cell
- with UXO, for the noise-free curve with low and moderate  $N_{pop}$
- with AXO, for noise-free and noisy data
- with AXO, for the benchmark cell with low and moderate  $N_{pop}$ .

This performance is a consequence of premature convergence, a well-known problem of EAs. As such, GAs with UXO or AXO are not appropriate for SC parameter extraction. On the other hand, GAs give very high accuracy when using BXO with a  $N_{pop}$  as small as 150, for all analyzed cases:

- For the noise-free curve, the parameter errors were smaller than  $10^{-13}\%$
- For noisy data, the parameter errors were smaller than 10% for practical cases, i.e. for noise up to 5%, and smaller than 30% for  $p$  up to 10%
- For the benchmark data, GAs gave the same RMSE as DEDCE [38], which has provided the smallest RMSE for this SC equal to  $7.730062 \times 10^{-4}$ .

It is important to note that the above results were reproduced in each of the 100 GA runs for each  $N_{pop}$  and had the same quality as the 5 methods considered in [13]. These results demonstrate that for SC parameter extraction, GAs with BXO should be classified at the top of the most efficient EAs. Previous studies carried out on clean data, concluded that GAs give bad precision or/and are not appropriate for SCs parameter extraction [1-4, 6, 39, 40]. This study used clean and noisy data, showing that if such conclusions are correct for UXO or AXO, they are not correct for BXO. Therefore, this study recommends the use of GA with BXO for SC parameter extraction. This result has to be confirmed with other OFs, other experimental data, and other XOs. Future works on EAs must study the effects of varying the genetic operators on the extracted parameters.

ACKNOWLEDGMENT

The authors acknowledge the support of the Directorate-General for Scientific Research and Technological Development (DGRSDT), Algeria. The software of this study

used the GALib genetic algorithm package, written by Matthew Wall at the Massachusetts Institute of Technology.

## REFERENCES

- [1] V. J. Chin, Z. Salam, and K. Ishaque, "Cell modelling and model parameters estimation techniques for photovoltaic simulator application: A review," *Applied Energy*, vol. 154, pp. 500–519, Sep. 2015, <https://doi.org/10.1016/j.apenergy.2015.05.035>.
- [2] D. T. Cotfas, P. A. Cotfas, and S. Kaplanis, "Methods to determine the dc parameters of solar cells: A critical review," *Renewable and Sustainable Energy Reviews*, vol. 28, pp. 588–596, Dec. 2013, <https://doi.org/10.1016/j.rser.2013.08.017>.
- [3] A. M. Humada, M. Hojabri, S. Mekhilef, and H. M. Hamada, "Solar cell parameters extraction based on single and double-diode models: A review," *Renewable and Sustainable Energy Reviews*, vol. 56, pp. 494–509, Apr. 2016, <https://doi.org/10.1016/j.rser.2015.11.051>.
- [4] R. Abbassi, A. Abbassi, M. Jemli, and S. Chebbi, "Identification of unknown parameters of solar cell models: A comprehensive overview of available approaches," *Renewable and Sustainable Energy Reviews*, vol. 90, pp. 453–474, Jul. 2018, <https://doi.org/10.1016/j.rser.2018.03.011>.
- [5] E. Batzeli, "Non-Iterative Methods for the Extraction of the Single-Diode Model Parameters of Photovoltaic Modules: A Review and Comparative Assessment," *Energies*, vol. 12, no. 3, Jan. 2019, Art. no. 358, <https://doi.org/10.3390/en12030358>.
- [6] A. R. Jordehi, "Parameter estimation of solar photovoltaic (PV) cells: A review," *Renewable and Sustainable Energy Reviews*, vol. 61, pp. 354–371, Aug. 2016, <https://doi.org/10.1016/j.rser.2016.03.049>.
- [7] M. Bashahu and P. Nkundabakura, "Review and tests of methods for the determination of the solar cell junction ideality factors," *Solar Energy*, vol. 81, no. 7, pp. 856–863, Jul. 2007, <https://doi.org/10.1016/j.solener.2006.11.002>.
- [8] S. Bader, X. Ma, and B. Oelmann, "One-diode photovoltaic model parameters at indoor illumination levels – A comparison," *Solar Energy*, vol. 180, pp. 707–716, Mar. 2019, <https://doi.org/10.1016/j.solener.2019.01.048>.
- [9] K. Bouzidi, M. Chegaar, and A. Bouhemadou, "Solar cells parameters evaluation considering the series and shunt resistance," *Solar Energy Materials and Solar Cells*, vol. 91, no. 18, pp. 1647–1651, Nov. 2007, <https://doi.org/10.1016/j.solmat.2007.05.019>.
- [10] F. Caracciolo, E. Dallago, D. G. Finarelli, A. Liberale, and P. Merhej, "Single-Variable Optimization Method for Evaluating Solar Cell and Solar Module Parameters," *IEEE Journal of Photovoltaics*, vol. 2, no. 2, pp. 173–180, Apr. 2012, <https://doi.org/10.1109/JPHOTOV.2011.2182181>.
- [11] X. Ma *et al.*, "Data-Driven I-V Feature Extraction for Photovoltaic Modules," *IEEE Journal of Photovoltaics*, vol. 9, no. 5, pp. 1405–1412, Sep. 2019, <https://doi.org/10.1109/JPHOTOV.2019.2928477>.
- [12] N. Maouhoub, "Photovoltaic module parameter estimation using an analytical approach and least squares method," *Journal of Computational Electronics*, vol. 17, no. 2, pp. 784–790, Jun. 2018, <https://doi.org/10.1007/s10825-017-1121-5>.
- [13] D. M. F  bba, E. C. Bortoni, A. F. Oliveira, and R. M. Rubinger, "The effects of noises on metaheuristic algorithms applied to the PV parameter extraction problem," *Solar Energy*, vol. 201, pp. 420–436, May 2020, <https://doi.org/10.1016/j.solener.2020.02.093>.
- [14] M. Mitchell, *An Introduction to Genetic Algorithms*. Cambridge, MA, USA: MIT Press, 1998.
- [15] W. Peng, Y. Zeng, H. Gong, Y. Leng, Y. Yan, and W. Hu, "Evolutionary algorithm and parameters extraction for dye-sensitized solar cells one-diode equivalent circuit model," *Micro & Nano Letters*, vol. 8, no. 2, pp. 86–89, 2013, <https://doi.org/10.1049/mnl.2012.0806>.
- [16] F. J. Toledo and J. M. Blanes, "Analytical and quasi-explicit four arbitrary point method for extraction of solar cell single-diode model parameters," *Renewable Energy*, vol. 92, pp. 346–356, Jul. 2016, <https://doi.org/10.1016/j.renene.2016.02.012>.
- [17] J. H. Holland, *Adaptation in Natural and Artificial Systems: An Introductory Analysis with Applications to Biology, Control, and Artificial Intelligence*. Cambridge, MA, USA: MIT Press, 1992.
- [18] K. Soleimani and J. Mazloum, "Designing a GA-Based Robust Controller For Load Frequency Control (LFC)," *Engineering, Technology & Applied Science Research*, vol. 8, no. 2, pp. 2633–2639, Apr. 2018, <https://doi.org/10.48084/etasr.1592>.
- [19] V. H. Nguyen, H. Nguyen, M. T. Cao, and K. H. Le, "Performance Comparison between PSO and GA in Improving Dynamic Voltage Stability in ANFIS Controllers for STATCOM," *Engineering, Technology & Applied Science Research*, vol. 9, no. 6, pp. 4863–4869, Dec. 2019, <https://doi.org/10.48084/etasr.3032>.
- [20] E. Jamalian and R. Foukerdi, "A Hybrid Data Mining Method for Customer Churn Prediction," *Engineering, Technology & Applied Science Research*, vol. 8, no. 3, pp. 2991–2997, Jun. 2018, <https://doi.org/10.48084/etasr.2108>.
- [21] J. Kingdon and K. Feldman, "Genetic algorithms and applications to finance," *Applied Mathematical Finance*, vol. 2, no. 2, pp. 89–116, Jun. 1995, <https://doi.org/10.1080/13504869500000006>.
- [22] R. Drechsler, *Evolutionary Algorithms for VLSI CAD*. Berlin, Germany: Springer Science & Business Media, 2013.
- [23] R. Drechsler and N. Drechsler, *Evolutionary Algorithms for Embedded System Design*. Norwell, MA, USA: Springer Science & Business Media, 2002.
- [24] V. Kumar and S. K. Dhull, "Genetic Algorithm based Optimization of Uniform Circular Array," *Engineering, Technology & Applied Science Research*, vol. 10, no. 6, pp. 6403–6409, Dec. 2020, <https://doi.org/10.48084/etasr.3792>.
- [25] M. Abdul-Niby, M. Alameen, A. Salhieh, and A. Radhi, "Improved Genetic and Simulating Annealing Algorithms to Solve the Traveling Salesman Problem Using Constraint Programming," *Engineering, Technology & Applied Science Research*, vol. 6, no. 2, pp. 927–930, Apr. 2016, <https://doi.org/10.48084/etasr.627>.
- [26] D. E. Goldberg, *Genetic Algorithms in Search, Optimization and Machine Learning*, 13th ed., Reading, MA, USA: Addison-Wesley Professional, 1989.
- [27] P. K. Singh, "A Modified Real-Coded Extended Line Crossover for Genetic Algorithm," in *Social Transformation – Digital Way*, Kolkata, India, 2018, pp. 702–716, [https://doi.org/10.1007/978-981-13-1343-1\\_58](https://doi.org/10.1007/978-981-13-1343-1_58).
- [28] F. Herrera, M. Lozano, and A. M. S  nchez, "A taxonomy for the crossover operator for real-coded genetic algorithms: An experimental study," *International Journal of Intelligent Systems*, vol. 18, no. 3, pp. 309–338, 2003, <https://doi.org/10.1002/int.10091>.
- [29] A. E. Eiben and J. E. Smith, *Introduction to Evolutionary Computing*. Berlin, Germany: Springer, 2015.
- [30] E. Wirsansky, *Hands-On Genetic Algorithms with Python: Applying genetic algorithms to solve real-world deep learning and artificial intelligence problems*. Birmingham, UK: Packt Publishing Ltd, 2020.
- [31] A. Sorsa, R. Peltokangas, and K. Leiviska, "Real-coded genetic algorithms and nonlinear parameter identification," in *2008 4th International IEEE Conference Intelligent Systems*, Varna, Bulgaria, Sep. 2008, vol. 2, <https://doi.org/10.1109/IS.2008.4670495>.
- [32] L. J. Eshelman and J. D. Schaffer, "Real-Coded Genetic Algorithms and Interval-Schemata," *Foundations of Genetic Algorithms*, vol. 2, pp. 187–202, Jan. 1993, <https://doi.org/10.1016/B978-0-08-094832-4.50018-0>.
- [33] "GALib: Matthew's Genetic Algorithms Library." <http://lancet.mit.edu/gal/>.
- [34] T. Easwarakhanthan, J. Bottin, I. Bouhouch, and C. Boutrif, "Nonlinear Minimization Algorithm for Determining the Solar Cell Parameters with Microcomputers," *International Journal of Solar Energy*, vol. 4, no. 1, pp. 1–12, Jan. 1986, <https://doi.org/10.1080/01425918608909835>.
- [35] A. Ferhat-Hamida, Z. Ouenoughi, A. Hoffmann, and R. Weiss, "Extraction of Schottky diode parameters including parallel conductance using a vertical optimization method," *Solid-State Electronics*, vol. 46, no. 5, pp. 615–619, May 2002, [https://doi.org/10.1016/S0038-1101\(01\)00337-9](https://doi.org/10.1016/S0038-1101(01)00337-9).

- 
- [36] J. H. Werner, "Schottky barrier and pn-junction I/V plots — Small signal evaluation," *Applied Physics A*, vol. 47, no. 3, pp. 291–300, Nov. 1988, <https://doi.org/10.1007/BF00615935>.
- [37] A. Askarzadeh and A. Rezazadeh, "Parameter identification for solar cell models using harmony search-based algorithms," *Solar Energy*, vol. 86, no. 11, pp. 3241–3249, Nov. 2012, <https://doi.org/10.1016/j.solener.2012.08.018>.
- [38] S. M. Parida and P. K. Rout, "Differential evolution with dynamic control factors for parameter estimation of photovoltaic models," *Journal of Computational Electronics*, vol. 20, no. 1, pp. 330–343, Feb. 2021, <https://doi.org/10.1007/s10825-020-01617-z>.
- [39] K. Ishaque, Z. Salam, H. Taheri, and A. Shamsudin, "A critical evaluation of EA computational methods for Photovoltaic cell parameter extraction based on two diode model," *Solar Energy*, vol. 85, no. 9, pp. 1768–1779, Sep. 2011, <https://doi.org/10.1016/j.solener.2011.04.015>.
- [40] N. Barth, R. Jovanovic, S. Ahzi, and M. A. Khaleel, "PV panel single and double diode models: Optimization of the parameters and temperature dependence," *Solar Energy Materials and Solar Cells*, vol. 148, pp. 87–98, Apr. 2016, <https://doi.org/10.1016/j.solmat.2015.09.003>.